TFY4345 Computational Assignment 1 - Projectile Motion

Marius Sunde Sivertsen
Studentnr: 478694

Svein Åmdal
Studentnr: 478704

September 2018

1 Introduction

With the following, we aim to answer the questions posed in the first numerical exercise in the course TFY4345 - Classical mechanics at NTNU, fall 2018.

We will perform a numerical simulation of two-dimensional projectile motion with air resistance. The equation of motion for such a system is given by Newton's 2nd law, and the equations can be decomposed into x- and y-directions. To solve the equations, we rewrite the second order system to a system of first-order differential equations, namely

$$\frac{\mathrm{d}x}{\mathrm{d}t} = v_x, \quad \frac{\mathrm{d}y}{\mathrm{d}t} = v_y, \quad \frac{\mathrm{d}v_x}{\mathrm{d}t} = -Dvv_x, \quad \frac{\mathrm{d}v_y}{\mathrm{d}t} = -Dvv_y - g, \tag{1}$$

for some altitude dependent drag coefficient $D = D(y)$, and $v = \sqrt{v_x^2 + v_y^2}$.

2 Exercise 1

2.1 Convergence test

To solve the differential equations numerically, we used the standard 4th order Runge-Kutta solver. This method uses a time-step iteration from an initial state. We want to make sure the implementation is correct, and get an estimate for a sufficiently small time increment dt between each step. If the implementation is correct, the numerical solution to any given problem should converge to the analytical solution, when dt decreases.

We choose a simple "dummy" problem where we know the analytical solution. By requiring conservation of energy in our problem, we can measure the difference between the energy of the analytical and numerical solutions, ΔE, and hope it decreases with decreasing dt. Total energy, E, is a particularly nice metric for convergence, as it requires both velocities and position to be calculated, and is therefore representative of all values we calculate numerically.

We re-use the algorithm from a planetary motion project[1], so it should be sufficient to show that the solver converges in the case of a planet orbiting the sun[2]. Instead of (1), the system of equations for a planetary orbit is

[1] Project 3 from the course TMA4320, spring 2018 - Planetary motion.

[2] It would have been more elegant to use a projectile throw with no air resistance as the "dummy" case, but we ran into practical issues with the implementation. Specifically, the values for the numerical and analytical energies were too similar, so ΔE produced a significant floating-point error (yes, we tried to allocate more memory to store each number, but to no avail).

$$\frac{dx}{dt} = v_x, \quad \frac{dy}{dt} = v_y, \quad \frac{dv_x}{dt} = -\frac{4\pi^2 x}{r^3}, \quad \frac{dv_y}{dt} = -\frac{4\pi^2 y}{r^3} \quad \text{where} \quad r = \sqrt{x^2 + y^2}, \tag{2}$$

however, the equations we solve should not effect the convergence. Figure 1 shows the mentioned energy

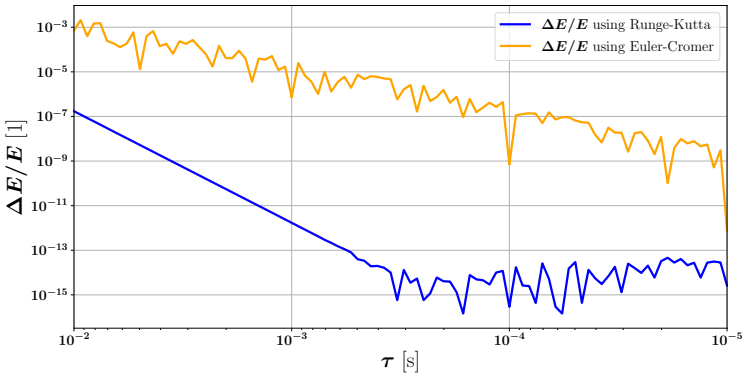

Figure 1: Convergence of numerical methods for a planetary orbit. The relative error in E done by the numerical method, decreases with decreasing $\tau = dt$. This implies convergence of the Runge-Kutta method in particular.

difference after one simulated orbit of the earth around the sun for different values of $\tau = dt$, as well as a bonus comparison against the same simulation run by the inferior Euler-Cromer algorithm.

In the figure, we have set the orbit period equal to 1, and it seems 5×10^{-2} s is a more than sufficient value of dt. Scaled to the order of magnitude we expect a projectile throw to last (upwards of 30 seconds), $dt = 5 \times 10^{-2}$ s should give more than sufficiently accurate numerical calculations for the projectile motions coming up. To justify the choice of the time step $dt = 5 \times 10^{-2}$ s we have included

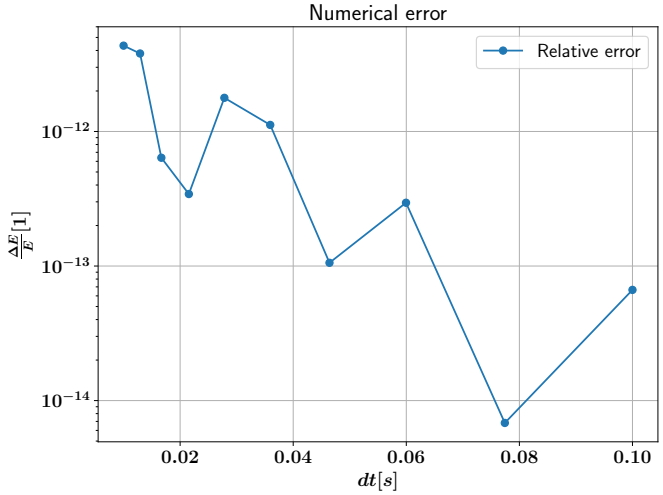

Figure 2: Numerical error by using the Runge-Kutta method of 4th order with different time steps dt. Here $\Delta E/E$ is the relative difference in the mechanical energy calculated numerically and analytically.

a plot of the numerical error in figure 2. Clearly, the numerical error with that time step is negligible compared to the precision we are interested in.

2.2 Air drag models

With $dt = 5 \times 10^{-2}\,\mathrm{s}$, we must consider some models for the air drag before we can calculate the trajectories. We assume throughout the calculations that we can model the force from air drag as $F_{drag} = -B_2 v^2$ to use as a basis for the drag coefficient D in (1).

No air drag

Assuming no air drag we simply set

$$D = 0$$

in the equations of motion (1).

isothermal drag model

For the isothermal drag model we consider a stationary amount of air with uniform temperature T under the influence of an uniform gravitational field. Assuming ideal gas law holds (accurate at high temperatures), then it follows that the *air density* ρ at any altitude y is

$$\rho(y) = \rho(0)e^{-y/h}, \qquad h = \frac{k_B T}{m_a g} \tag{3}$$

where k_B is Boltzmann's constant, m_a is the average mass of an air particle and g is the constant acceleration due to gravity.

Assuming the drag force is proportional to the density relative to $\rho(0)$, we then find that

$$D(y) = \frac{B_2}{m} e^{-y/h}$$

in the equations of motion (1).

Adiabatic drag model

For the adiabatic drag model we consider the density change of an amount of air during an adiabatic process. Using again ideal gas law and the first law of thermodynamics, it follows that the air density ρ at any altitude y is

$$\rho(y) = \rho(0)\left(1 - \frac{ay}{T_0}\right)^{\alpha}, \tag{4}$$

where a is the temperature gradient, T_0 is the temperature at sea level and α is the adiabatic constant of air.

Again assuming the drag force is proportional to the density relative to $\rho(0)$, we find that

$$D(y) = \frac{B_2}{m}\left(1 - \frac{ay}{T_0}\right)^{\alpha}$$

in the equations of motion (1).

2.3 Trajectories and optimal angles

As we see in figure 3, the different air drag models significantly effect the trajectory for a given initial state. As such, it seems likely that the firing angle (between initial velocity and positive x-axis) might be different for the different models. We now desire the *optimal angle* such that the firing range is maximal (distance covered in x-direction). To achieve this, we numerically calculated the range for many different angles and selected the angles with the largest range[3]. A plot of the ranges for different firing angles can

[3] A more rigorous way to really approach the maximum would be to solve the equation $dx(\theta)/d\theta = 0$ with something like a one-dimensional gradient descent algorithm. We argue, however, that for a large enough selection of firing angles, the method we used gives a good enough approximation.

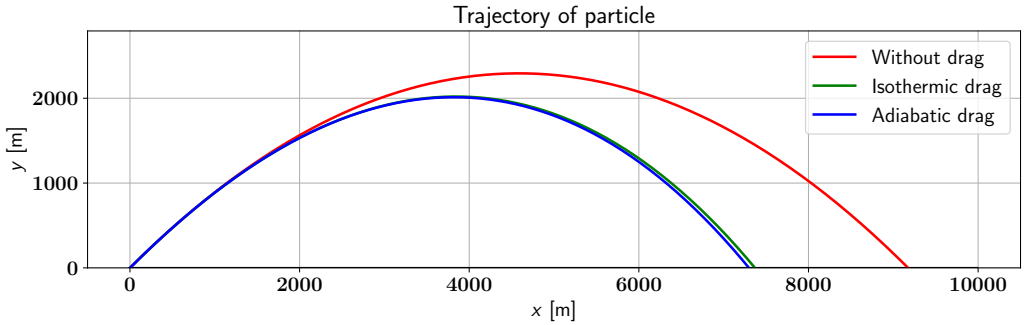

Figure 3: Plots of the trajectories for different air drag models, using the starting state with $v_0 = 700m/s$ and $\theta = 45^o$.

be seen in figure 4. Keeping the starting velocity as before ($v_0 = 700\,\mathrm{m\,s^{-1}}$), we obtain the optimal firing angles to be 44.9° for no air drag[4], 43.94^o for isothermal drag, and 43.60^o for adiabatic drag. Figures

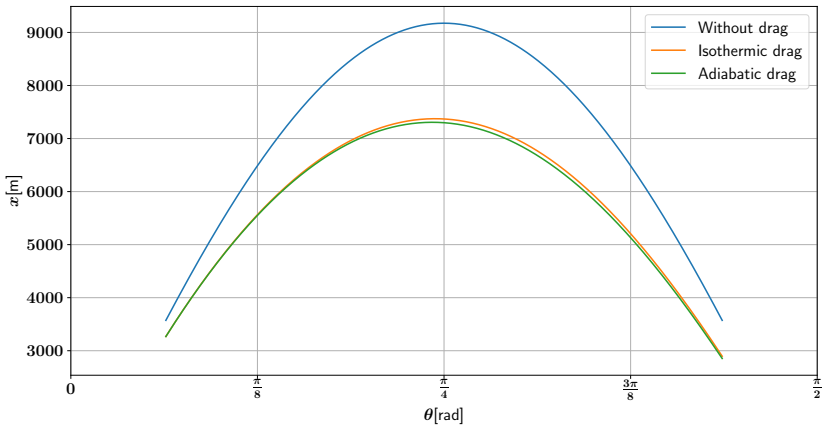

Figure 4: The range, x, for different firing angles, θ using our air drag models. The starting velocity is the same as before, $v_0 = 700m/s$.

5, 6 and 7 shows the trajectories of the optimal firing angles, as well as two other angles for all the air drag models. Qualitatively, this should give some idea of why the optimal angle is what it is.

[4]Analytically, this angle should be 45^o. As discussed in an earlier footnote, the selection of optimal angles are not perfected, but good enough to get an idea how the air drag changes the trajectory.

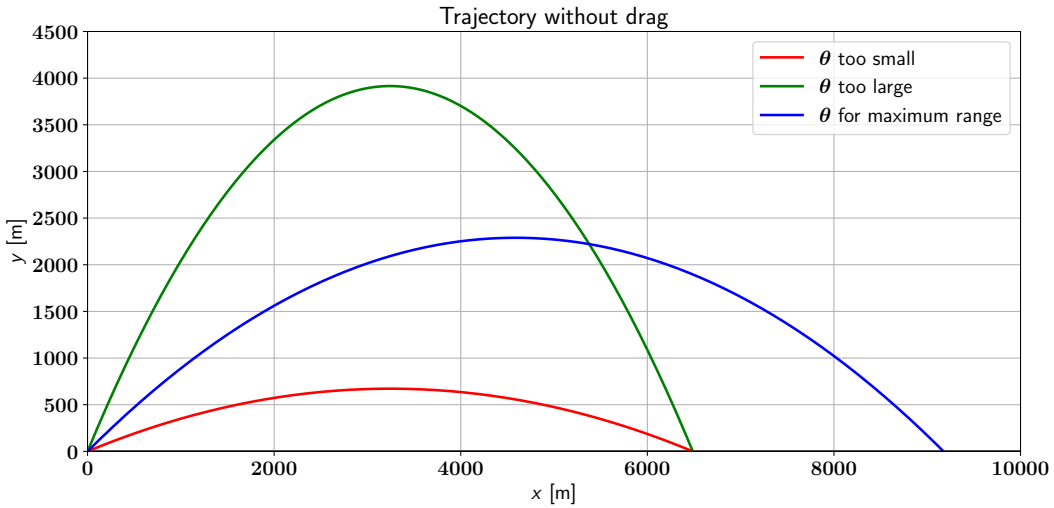

Figure 5: Trajectories for some firing angles using no air drag.

3 Exercise 2

3.1 The Big Bertha Gun

The trajectory analysis from the previous section can now be used to model a trajectory of a specific grenade that were launched by the considerably big German gun, Bertha. We assume that the muzzle exit speed of the grenade is $1630\,\mathrm{m\,s^{-1}}$, and that the grenade mass is 106 kg. We do the same as before, and find a good approximation for the optimal angle. Using the adiabatic drag model, we plot the range for a few angles in fig 8, and find that the optimal angle is 51.5°. Figure 9 shows the trajectory of the grenade shell that maximises the range given the initial conditions mentioned above. The maximal range of the grenade is here calculated to be approximately 148 km, with the apogee located 49.5 km above the firing range with an air time of 201 s.

4 Summary

We have numerically solved the system of differential equations given by (1) to obtain the trajectories of projectiles, taking air resistance into account. Finally, we simulated the trajectory and range of an actual cannon, and found the maximal possible range of the cannon to be 148 km (this is a remarkable range compared to other cannons during world war 1!).

5 Final thoughts

In the next project, we will interpret the convergence test differently. The shortcoming of the model used here, is that it does not show anything for situations where energy is not conserved (i.e. projectile motion with drag). An improvement here would be to simply compare the output of the simulation using two different time steps, and check that the difference between them vanishes as $dt \to 0$.

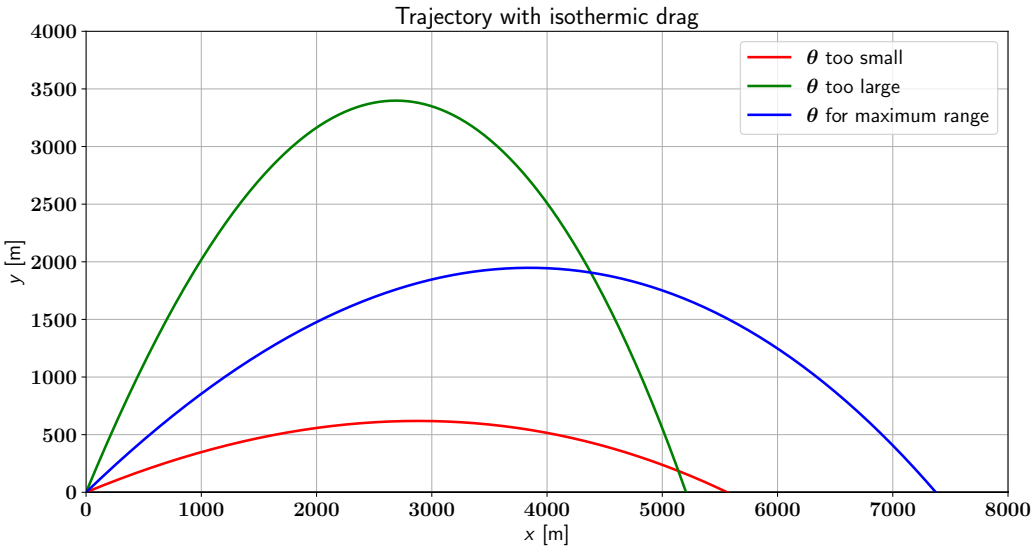

Figure 6: Trajectories for some firing angles using the isothermal air drag model.

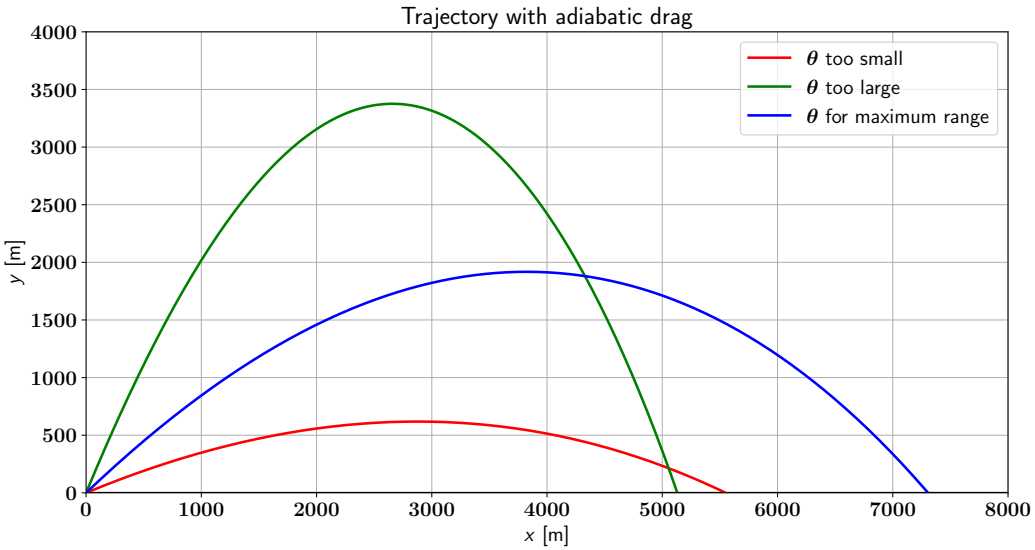

Figure 7: Trajectories for some firing angles using the adiabatic air drag model.

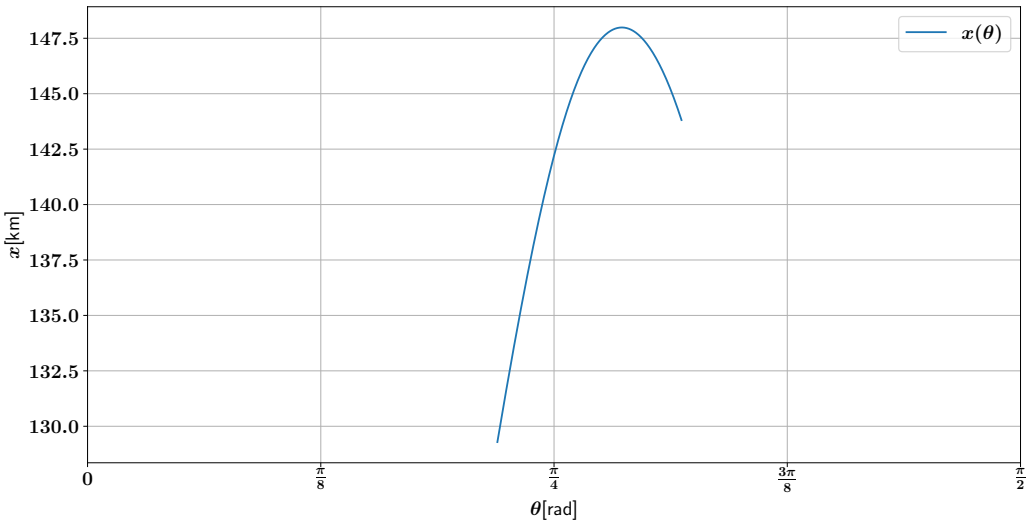

Figure 8: This plot shows the range x of the Bertha gun as a function of the initial launch angle θ

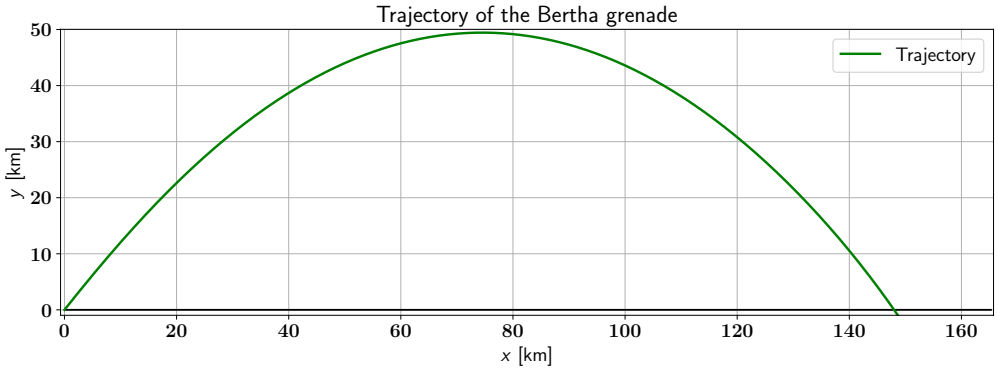

Figure 9: The trajectory of the grenade shell.